ISSN 1070-3632, Russian Journal of General Chemistry, 2018, Vol. 88, No. 12, pp. 2550–2558. © Pleiades Publishing, Ltd., 2018.
Original Russian Text © V.G. Vlasenko, A.S. Burlov, T.A. Kuz'menko, A.T. Kozakov, A.V. Nikol'skii, A.L. Trigub, S.I. Levchenkov, 2018, published in Zhurnal Obshchei Khimii, 2018, Vol. 88, No. 12, pp. 2034–2043.

Synthesis, Structure, and X-Ray Photoelectron Spectra of Cobalt and Copper Complexes with 2-{(*E*)-[2-(4-Hydroxybutylamino)benzimidazol-1-yl]iminomethyl}phenol

V. G. Vlasenko[a]*, A. S. Burlov[b], T. A. Kuz'menko[b], A. T. Kozakov[a], A. V. Nikol'skii[a], A. L. Trigub[c], and S. I. Levchenkov[d]

[a] *Research Institute of Physics, Southern Federal University, pr. Stachki 194, Rostov-on-Don, 344090 Russia*
**e-mail: v_vlasenko@rambler.ru*

[b] *Research Institute of Physical and Organic Chemistry, Southern Federal University, Rostov-on-Don, Russia*

[c] *"Kurchatov Institute" National Research Center, Moscow, Russia*

[d] *Southern Research Center, Russian Academy of Sciences, Rostov-on-Don, Russia*

Received May 8, 2018
Revised May 8, 2018
Accepted May 11, 2018

Abstract—A new azomethine compound, 2-{(*E*)-[2-(4-hydroxybutylamino)benzimidazol-1-yl]iminomethyl}-phenol, and its cobalt(II) and copper(II) complexes were synthesized and characterized by IR, ^{1}H NMR, and X-ray photoelectron spectroscopy and quantum-chemical calculations. The crystal and molecular structures of the cobalt complex were established by X-ray diffraction analysis. The oxidation state of the cobalt ion in the complex after its crystallization from the solution was defined more exactly by X-ray photoelectron spectroscopy.

Keywords: azomethines, metal chelates, cobalt(II) complexes, X-ray absorption spectroscopy

DOI: 10.1134/S1070363218120150

Bezimidazole derivatives, azomethine and azo compounds containing a benzimidazole fragment, as well as their metal complexes are being vigorously studied [1, 2]. They exhibit broad-spectrum biological and chemisensing activities [3–7]. The azomethine derivatives of 2-hydroxy- and 2-tosylaminobenzaldehydes and aminoazoles [8–12], as well as 2-hydroxy- and 2-phenylaminoazobenzimidazoles [13, 14] are potential polydententate ligand systems. They have a few donor centers and, therefore, can serve as fruitful models for studying competitive coordination of metals to different donor centers in ligands systems in mono- and polynuclear complexes [15].

Scarce data are available on metal complexes with the azomethine derivatives of 2-hydroxy- and 2-tosylaminobenzaldehydes and *N*-aminoazoles. The possibility of synthesis of mono- and binuclear complexes with such ligands was demonstrated [8–12, 16]. Heterocyclic ligands with benzimidazole or imidazole fragments and their mononuclear and polynuclear complexes were found to show the greatest promise [17–26].

We synthesized 2-{(*E*)-[2-(4-hydroxybutylamino)-benzimidazol-1-yl]iminomethyl}phenol **1** and its cobalt(II) and copper(II) complexes. Azomethine **1**, a derivative of 2-hydroxybenzaldehyde and 4-(1-aminobenzimidazol-2-ylamino)butan-1-ol, is potential tetradentate ligand capable of forming complexes of different compositions and structures. Compound **1** can exist both as an amine **1A** and in an imine tautomer **1B** (Scheme 1) [8].

To evaluate the relative stability of the tautomeric forms of azomethine **1**, we performed B3LYP/TZVP DFT calculations of their total energies and electronic

Scheme 1.

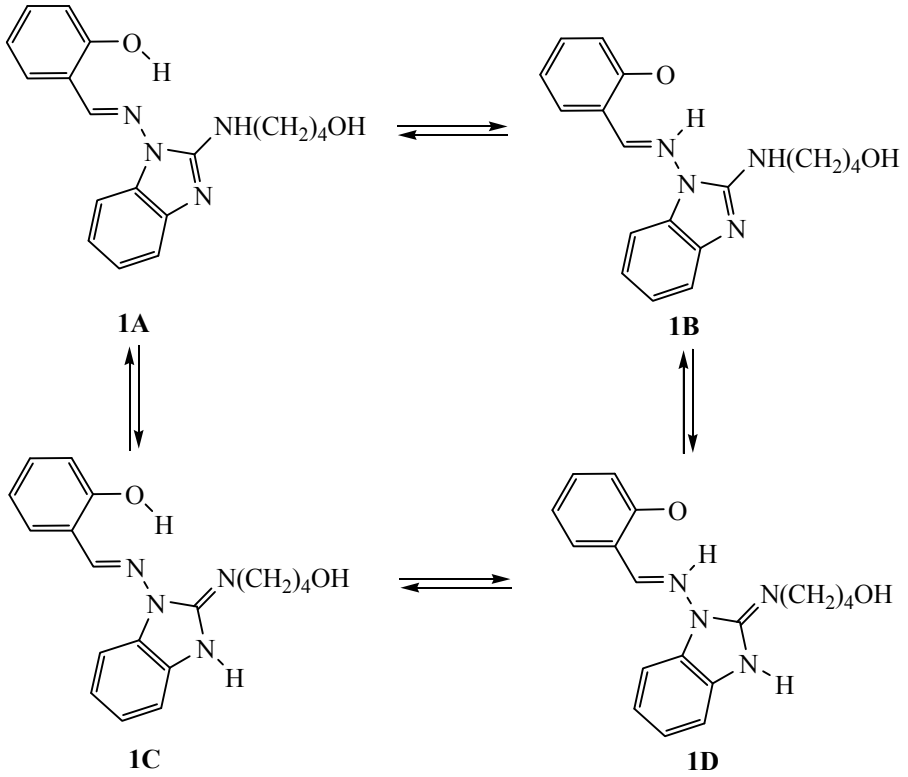

and steric structures [27–29]. Full geometry optimization with no symmetry constraints was applied.

Tautomer **1A** is the most stable form of azomethine **1** (Scheme 1). Benzimidazol-2-imine tautomer **1B** is destabilized with respect to form **1A** in a vacuum by as little as 1.4 kcal/mol. Tautomers **1B** and **1D** are higher in energy in a vacuum than tautomer **1A** by 7.3 and 13.6 kcal/mol, respectively.

The composition and structure of azomethine **1** (H_3L) were established by elemental analysis and IR and ^{1}H NMR spectroscopy. The ^{1}H NMR spectrum of compound **1** displays alcoholic and phenolic OH proton signals at 4.48 and 10.28 ppm, respectively. The NH proton signals appear in the aromatic proton region at 6.95–7.10 ppm and the CH=N proton signals appear at 9.20 ppm. The IR spectrum of compound **1** contains broad weak absorption bands at 3511 (N–H) and 3356 cm^{-1} (O–H) and strong bands at 1621 and 1602 cm^{-1} (CH=N).

The cobalt(II) and copper(II) complexes were synthesized by reacting azomethine **1** dissolved in a 2 : 1 mixture of methanol and DMF and methanolic cobalt acetate tetrahydrate or copper acetate monohydrate (Scheme 2).

According to the elemental analysis, cobalt complex **2a** isolated from the reaction mixture has the composition $M(HL)_2$. Its IR spectrum no longer contains the ν(N–H) band, and the weak broad OH band is observed at 3315 cm^{-1}. The strong ν(CH=N) band at 1618 cm^{-1} is slightly weaker compared to complex **1**. Complex **2a** is paramagnetic [μ_{eff} = 4.3 B.M. (294 K)]. Such magnetic moment is characteristic of high-spin octahedral (d^2sp^3) cobalt(II) complexes and points suggests a mononuclear structure of complex **2a**.

The elemental analysis of copper complex **2b** allows it to be assigned the composition $CuHLCH_3COO$. The IR spectrum of complex **2b** shows a broad weak absorption band of the N–H and O–H bonds in the range 3600–3000 cm^{-1}, a strong acetate C=O band at 1675 cm^{-1}, and strong ν(CH=N) bands at 1622 and 1600 cm^{-1}. The μ_{eff} is 1.97 B.M. (294 K) and scarcely changes with decreasing temperature, which points to a mononuclear structure of the complex.

The local atomic structure of complexes **2a, b** was established by X-ray photoelectron spectroscopy from an analysis of the Co*K*- and Cu*K*-edge XANES and

Scheme 2.

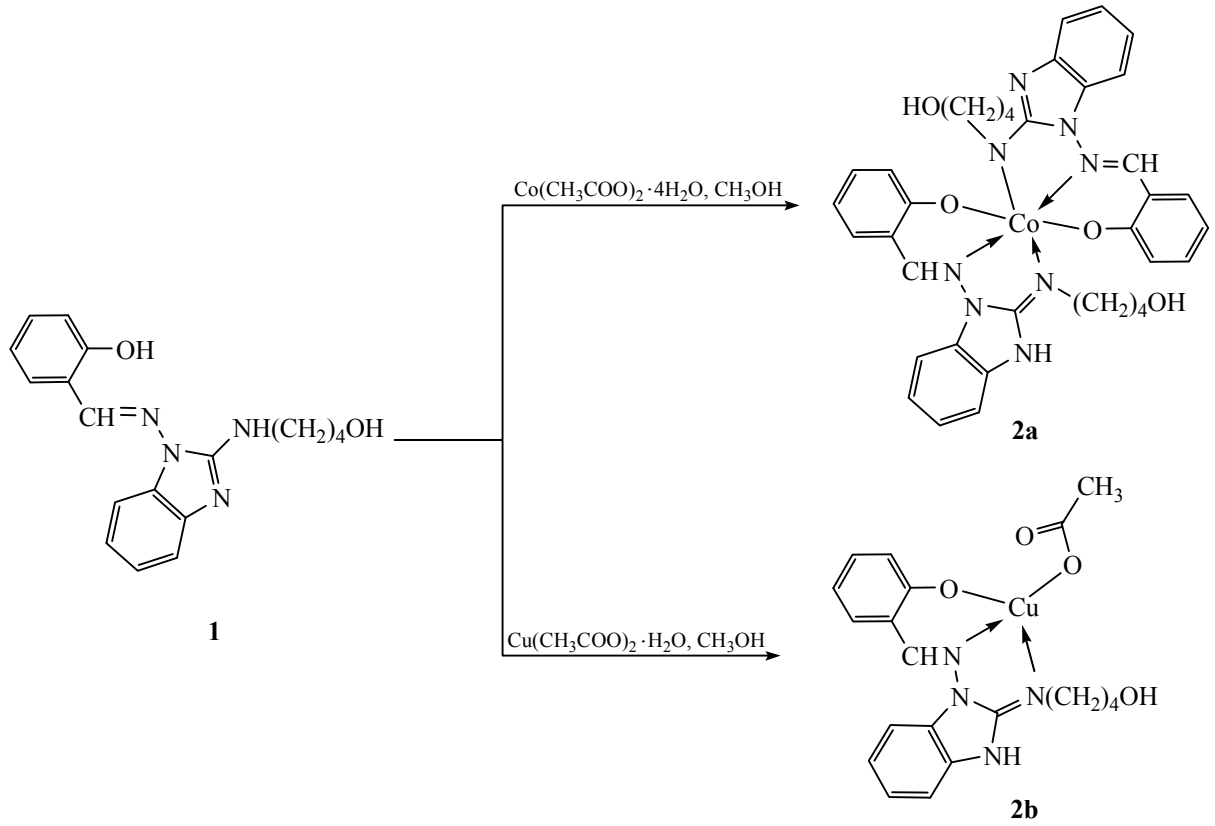

EXAFS spectra. Figures 1a and 1b show the normalized Co*K*- and Cu*K*-edge XANES spectra of complexes **2a**, **2b**, and the inserts show the first derivatives $d\mu/dE$ of these spectra. The XANES spectrum of complex **2a** contains a main peak *C* due to $1s \rightarrow 4p^*$ transitions and a weak pre-edge peak *A*. The latter peak can be due to *p–d*-mixing of metal AOs (in the case of a low-symmetry metal environment) or due to exclusively quadrupole transitions (for example, in the case of an octahedral metal environment). As judged from the XANES spectrum of complex **2a**, where the pre-edge peak *A* is very weak, in our case the second option is most likely. When the cobalt ion in complex **2a** has an octahedral environment, the first derivative of the Co*K*-edge XANES spectrum displays a narrow single maximum because of the degeneration of vacant $4p^*$ orbitals of Co. At the same time, the experimental $d\mu/dE$ derivative shows a slight splitting, suggesting a distorted geometry of the coordination entity in this complex.

The Cu*K*-edge XANES spectrum of complex **2b** and its $d\mu/dE$ derivative have patterns characteristic a square-planar environment of the absorbing copper ion. Evidence is provided first of all by the presence of a well-defined shoulder *B* directly in the Cu*K*-edge curve, which corresponds to the $4p_z^*$-AO of the metal, as well as by the low intensity of the pre-edge peak *A*, which is explained by the absence of inversion center in a square-symmetric coordination center. The first $d\mu/dE$ derivative of the Cu*K* edge XANES spectrum, too, displays two well-defined maxima due to splitting of the copper $4p_z^*$-, $4p_x^*$-, and $4p_y^*$-AOs.

The quantitative characteristics of the local atomic structures of complexes **2a**, **2b** were obtained from the *K*-edge EXAFS X-ray absorption spectrum spectra. Figures 1c and 1d present the EXAFS FTM curves for the complexes. The spectra both contain their main peaks at r = 1.48–1.53 Å, but the FTM amplitude of this peak for complex **2a** is much smaller than for complex **2b**. According to the suggested model of the coordination entity, the main peak corresponds to photoelectron scattering on the first coordination sphere comprising the oxygen and nitrogen atoms of the ligand.

The theoretical calculations of the EXAFS spectra of complexes **2a**, **2b** allowed us to determine the characteristics of the closest environment of the metal

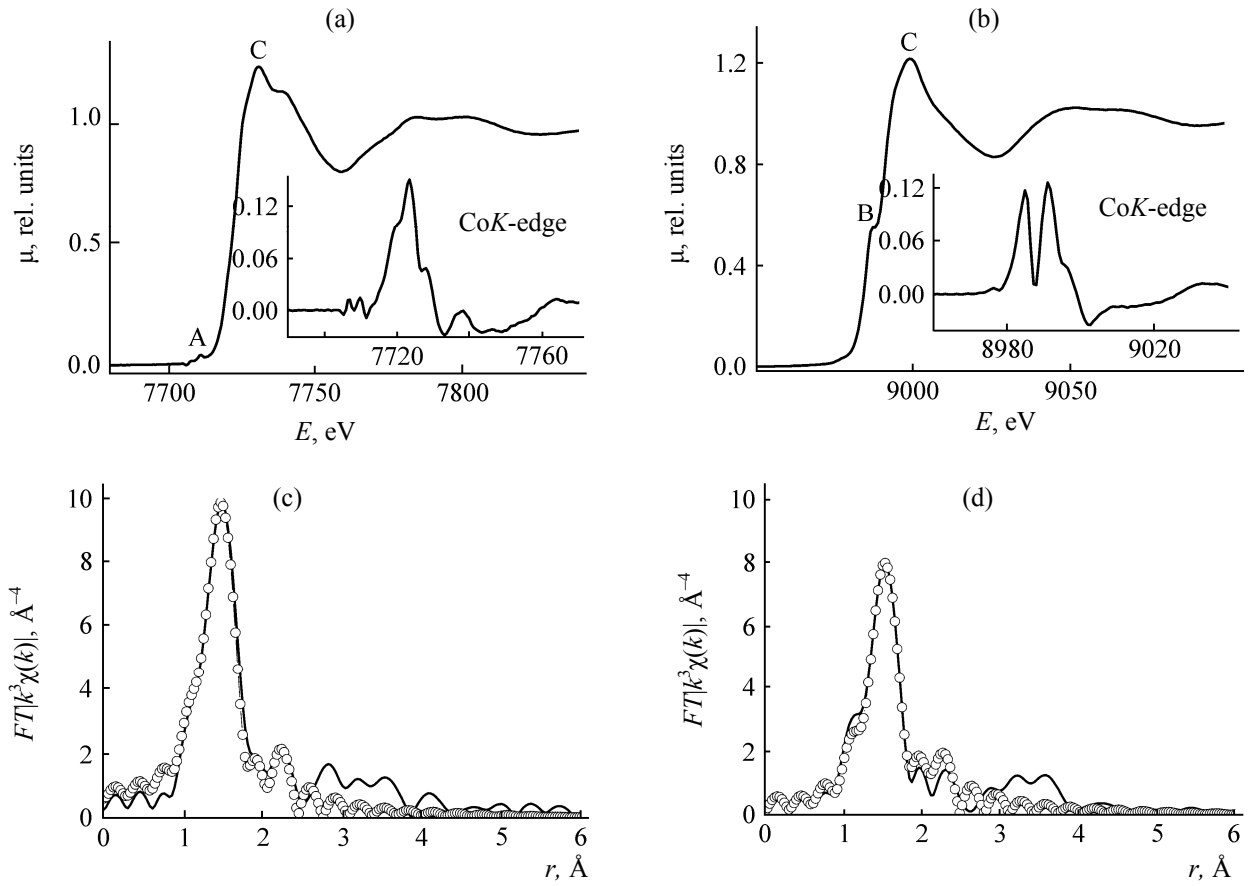

Fig. 1. (a, b) Normalized XANES spectra and corresponding first derivatives $d\mu/dE$ and (c, d) Co*K*- and Cu*K*-edge EXAFS FTM curves for complexes (a, c) **2a** and (b, d) **2b**.

ions in the complexes, and for the criterion of the best models we chose the minimal value of the *Q*-factor (Table 1). As seen from the data in Table 1, even though the complexes have close Debye–Waller factors, the coordination number of cobalt in complex **2a** is 6, whereas the coordination number of copper in complex **2b** is 4, which is consistent with the qualitative conclusions based on the XANES spectral data. The average distances to the first coordination sphere are close to values typical of similar complexes. Considering the resulting coordination number for complex **2b**, we suggested that the central atom in it coordinates one azomethine ligand **1** and one acetate group (half-acetate complex). The possible formation of dimeric molecules does not take place, which follows from the absence of a peak corresponding to the Cu···Cu distance from the EXAFS FTM curve for complex **2b**.

The conclusions on the octahedral geometry of complex **2a** and square-planar geometry of complex **2b** agree with the magnetochemical data and elemental analyses.

Table 1. Parameters of the local atomic environment of the metal ions in complexes **2a**, **2b**[a]

Comp. no.	*N*	*r*, Å	σ^2, Å^2	CS	*Q*, %[b]
2a	4	1.90	0.0039	O/N	2.3
	2	1.95	0.0039	O/N	
2b	4	1.97	0.0036	O/N	2.9

[a] (*r*) Interatomic distance; (*N*) coordination number; (σ^2) Debye–Waller factor; (CS) coordination sphere; $Q(\%) = \frac{\Sigma[k\chi_{exp}(k) - k\chi_{th}(k)]^2}{\Sigma[k\chi_{exp}(k)]^2} \times 100\%$ – goodness-of-fit function. [b] Approximation range in the *r*-space Δr = 1.0–2.0 Å.

Table 2. Principal interatomic distances and valence angles in the coordination polyhedra of cobalt in complex **2c**

Bond	*d*, Å	Bond	*d*, Å
$Co^1–N^1$	1.901(2)	$Co^1–N^5$	1.905(2)
$Co^1–N^4$	1.938(2)	$Co^1–N^8$	1.923(2)
$Co^1–O^1$	1.890(2)	$Co^1–O^3$	1.921(2)
Angle	α, deg	Angle	α, deg
$O^1Co^1N^1$	94.22(7)	$N^5Co^1N^8$	84.68(8)
$O^1Co^1N^5$	87.45(7)	$O^3Co^1N^8$	177.61(7)
$N^1Co^1N^5$	177.67(8)	$O^1Co^1N^4$	178.59(7)
$O^1Co^1O^3$	89.00(7)	$N^1Co^1N^4$	84.38(7)
$N^1Co^1O^3$	88.64(7)	$N^5Co^1N^4$	93.95(7)
$N^5Co^1O^3$	93.01(7)	$O^3Co^1N^4$	90.75(7)
$O^1Co^1N^8$	90.25(7)	$N^8Co^1N^4$	90.05(8)
NCo^1N^8	93.69(8)		

Slow crystallization of complex **2a** from a DMF solution gave its single-crystalline sample. By the results of XRD analysis, the sample was assigned the composition [CoL(HL)] (complex **2c)**, with the mono- and double-deprotonated azomethine **1** fragments coordinated to the cobalt(III) ion in a tridentate fashion (Fig. 2). The coordination polyhedron of the cobalt ion can be described as a distorted octahedron formed by the phenoxide O^1 and O^3, azomethine N^1 and N^5, and amine N^4 and N^8 atoms. The $Co^1–N^1$ and $Co^1–N^5$ bond lengths are quite close to each other [1.901(2) and 1.905(2)Å, Table 2], while the $Co^1–N^4$ and $Co^1–N^8$ bond lengths differ from each other by 0.015 Å [1.938(2) and 1.923(2)Å]. The difference in the $Co^1–O^1$ and $Co^1–O^3$ bond lengths is even larger and makes 0.031Å [1.890(2) and 1.921(2) Å, respectively], which is likely explained by the different degrees of deprotonation of the azomethine ligands. The alkylamino group proton in the monodeprotonated ligand passes to the benzimidazole N^3 atom on coordination.

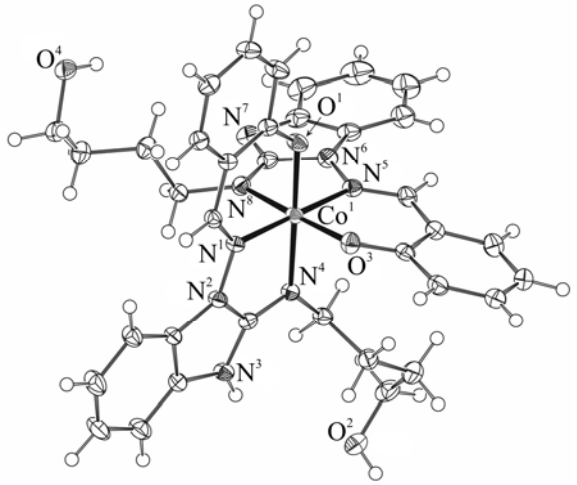

Fig. 2. General view of a molecule of complex **2 c** (thermal ellipsoids are given at a 50% probability level).

Both five-membered metal-chelate cycles and the six-membered $Co^1O^1C^1C^6C^7N^1$ cycle formed by the monodeprotonated ligand are almost planar. The six-membered $Co^1O^3C^{19}C^{24}C^{25}N^5$ metal-chelate cycle is slightly distorted, because the O^3 and C^{19} atoms deviate from the rms plane formed by the other atoms by 0.325 and 0.151 Å, respectively. The selected interatomic distances and bond angles in complex **2c** are listed in Table 2.

The presence in the single-crystalline complex **2c** of both two OH groups not involved in coordination to the metal ions and the NH group of the protonated benzimidazole fragment results in that each molecule of the complex forms 3 intermolecular hydrogen bonds with two neighboring molecules: $O^2–H^{2A\cdots}N^{7i}$, $N^3–H^{3B\cdots}O^{4i}$, and $O^4–H^{4A\cdots}O^{2ii}$ [crystallographic positions: (*i*) *x*–1, *y*, *z*; (*ii*) *x*+1, *y*, *z*]. The single crystal of the complex contains infinite chains of hydrogen-bonded molecules running along the *a* axis (Fig. 3). Table 3 lists the characteristics of hydrogen bonds in single crystal **2c**.

Thus, the results of XRD analysis slightly contradict the results of elemental analysis, IR spectroscopy, and magnetochemical measurements. We suggested that, as the single crystal is growing, atmospheric oxygen oxidizes Co(II) to Co(III). To check the oxidation state of cobalt, we have measured the X-ray photoelectron spectra (XPS) of fine crystals of a freshly prepared powder of complex **2a** and single crystal **2c**. The shapes and energy characteristics of the XPS spectra of core shells of 3*d* metals in compounds depend of the valence state of the transition metal and the degree of covalency of its chemical bonds. Figure 4 shows the XPS Co-2*p* spectra of the two samples. Both spectra show main peaks (A and B) corresponding to the spin-orbit components Co $2p_{3/2,1/2}$. Furthermore, each of the main peaks is accompanied high-energy satellite bands C and D associated with charge transfer from the ligand to metal, specifically, to its lower vacant orbitals which have predominantly 3*d* character. The intensity of the satellite peaks is highly sensitive to the oxidation state of the metal ion: they are relatively weak with Co(III) and double as intense

with Co(II) [30]. The XPS data allow us to state that the oxidation state of cobalt in the single-crystalline complex **2c** is +3, whereas the fine-crystalline powder isolated from the reaction mixture contains Co(II) and, probably, a small admixture of Co(III). The complete oxidation of Co(II) to Co(III) in the single crystal is likely to occur as it is growing from the solution for a long time in air; in the fine crystals of complex **2a**, partial oxidation to form a Co(III)/Co(II) mixture takes place during XPS measurements.

EXPERIMENTAL

The attenuated total internal reflectance IR spectra were obtained on a Varian Excalibur-3100 FTIR instrument for powders. The ^{1}H NMR spectra were registered on a Varian Unity-300 spectrometer (300 MHz) for $CDCl_3$ solutions. The chemical shifts were measured against residual proton signals of the deuterated solvent. The CHN elemental analysis was performed on a Carlo Erba Instruments TCM 480 analyzer. Analysis for metals was performed by gravimetry.

The solid-phase specific magnetic susceptibilities were measured on a Faraday balance at room temperature in a magnetic field of 9 kOe (atomic diamagnetism was included by the Pascal scheme) [31]. The effective magnetic moment (μ_{eff}) was calculated by Eq. (1).

$$\mu_{eff} = \sqrt{\left(\frac{3k}{N}\mu_B\right)\chi T} \approx \sqrt{8\chi T}. \quad (1)$$

Here k is the Boltzmann constant; N, Avogadro number; and μ_B, Bohr magneton.

Table 3. Characteristics of hydrogen bonds in complex **2c**[a]

D–H···A	D–H, Å	H···A, Å	D···A, Å	∠DHA, deg
O^2–H^{2A}···N^{7i}	0.824(17)	1.914(19)	2.700(3)	159(3)
N^3–H^{3B}···O^{4i}	0.880	1.890	2.763(3)	169(3)
O^4–H^{4A}···O^{2ii}	0.84(2)	1.83(2)	2.659(3)	175(3)

[a] Crystallographic positions: (*i*) *x*–1, *y*, *z*; (*ii*) *x*+1, *y*, *z*.

The Co*K*- and Cu*K*-edge X-ray absorption spectra were obtained in the transmission mode on an EXAFS spectrometer at the Structural Materials Science End-Station, Kurchatov Center for Synchrotron Radiation and Nanotechnology, Moscow. The energy of the electron beam used as a source of X-ray synchrotron radiation was 2.5 GeV at an average current of 80–120 mA. The X-ray absorption spectra were processed by standard procedures involving background subtraction, *K*-edge-step normalization, and atomic absorption background μ_0 subtraction, after which Fourier transform of the obtained EXAFS (χ) spectrum was performed in the range of photoelectron wave vectors k from 2.5 to 12–13 Å^{-1} with the weight function k^3. The resulting EXAFS FTM corresponded, to a phase-shift accuracy, to the radial distribution function of atoms around the absorbing metal ion. The exact parameters of the immediate environment of the cobalt and copper ions in the studied compounds were obtained by nonlinear least-squares fit of the parameters of the corresponding coordination spheres obtained from the calculated EXAFS spectrum and the Fourier-filtered total X-ray absorption spectrum, using the IFFEFIT suite of programs [32]. The photoelectron scattering phases and amplitudes required for

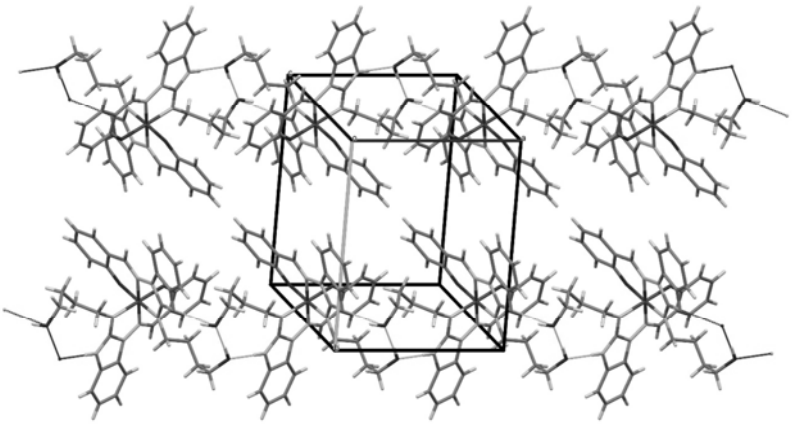

Fig. 3. Infinite chains of hydrogen-bonded molecules in the single-crystalline complex **2c** (view along the crystallographic axis *c*).

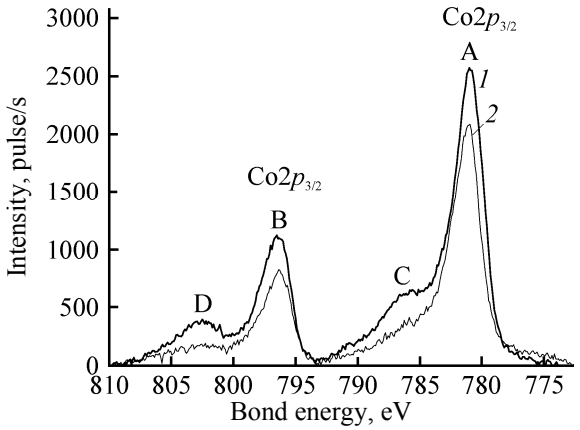

Fig. 4. Co 2*p* X-ray photoelectron spectra of complexes (*1*) **2a** and (*2*) **2c**.

calculating the model spectrum were calculated by the FEFF7 program [33]. The XRD data for single crystal **2c** were used as the input atomic coordinates for calculating scattering phases and amplitudes and further fitting.

The XRD analysis was performed on a Bruker SMART APEX2 CCD diffractometer (MoK_α, λ = 0.71073 Å, graphite monochromator, ω-scanning). The measured intensities were processed using the SAINT and SADABS programs included in the APEX2 suite of programs [34, 35]. The structures were solved by the direct method and refined by full-matrix least squares (on F^2_{hkl}.) with anisotropic temperature factors for non-hydrogen atoms. Hydrogen atoms were placed in geometrically calculated positions. All calculations were performed using the SHELXTL suite of programs [36]. The experimental details and crystal data are given in Table 4. Analysis of the structures was performed using the PLATON program [37]. The atomic coordinates and temperature factors are deposited at the Cambridge Crystallographic Data Center (CCDC 1840083).

The X-ray photoelectron (XPE) spectra the single-crystalline complex **2c** and powdered complex **2a** were measured using an ESCALAB 250 X-ray photoelectron microprobe with a monochromatic AlK_α X-ray source. The absolute resolvable energy range was 0.5 eV (by the Ag $3d_{5/2}$ line). The X-ray spot diameter on the sample was 500 μm, which was sufficient for measurements. To remove the positive charge, the samples were irradiated simultaneously by slow electrons and ions. The surface of the single crystal was purified with a diamond broach file in a

Table 4. Crystal data and experimental and structure refinement parameters for complex **2c**

Parameter	Value	Parameter	Value
Brutto formula	$C_{36}H_{37}CoN_8O_4$	d_{calc}, g/cm^3	1.428
M	704.67	μ, mm^{-1}	0.58
Crystal dimensions, mm	0.34 × 0.23 × 0.13	*F*(000)	736
Temperature	153(2)	θ range, deg	2.1–28.2
Syngony	Triclinic	Index ranges	–13< *h* < 12, –16< *k* < 15, –0< *l* < 18
Space group	*P*-1	Measured reflections	7485
a, Å	10.0293(6)	Unique reflections	7467
b, Å	12.4896(7)	Reflections with $I > \sigma(I)$	6412
c, Å	14.2246(8)	Refinement variables	451
α, deg	104.6380(8)	*GOOF* (all reflections)	1.000
β, deg	105.5071(8)	R_1 [$I > 2\sigma(I)$]	0.041
γ, deg	94.7771(8)	wR_2 (all reflections)	0.114
V, Å^3	1639.32(16)	$\Delta\rho_{max}/\Delta\rho_{min}$, *e*/Å^3	0.455/–0.392
Z	2		

sample preparation chamber at a pressure of ~1× 10^{-6} Pa.

Commercially available salicylaldehyde, cobalt(II) acetate tetrahydrate, and copper(II) acetate monohydrate were used. 4-(1-Aminobenzimidazol-2-ylamino)butan-1-ol was synthesized as described in [38].

2-[(*E*)-[2-(4-Hydroxybutylamino)benzimidazole-1-yl]iminomethyl]phenol (H_3L, 1). A solution 0.88 g (4 mmol) of 4-(1-aminobenzimidazol-2-ylamino)butan-1-ol and 0.49 g (4 mmol) of salicylaldehyde in 20 mL of toluene was heated under reflux for 3 h. After cooling, the precipitate was filtered off, washed with hexane, and recrystallized from butn-1-ol. Yield 1.24 g (76%), colorless crystals, mp 214–215°C. IR spectrum, ν, cm^{-1}: 3511 br. w (NH), 3356 br. w (O–H), 1621 m (C=N), 1602 s. ^{1}H NMR spectrum (DMSO-d_6), δ, ppm: 1.48–1.70 m (4H, CH_2), 3.29–3.48 m (4H, CH_2), 4.48 t (1H, OH, J = 1.2 Hz), 6.95–7.10 m (5H_{Ar}, NH), 7.27 d (1H_{Ar}, J = 7.5 Hz), 7.35 t (1H_{Ar}, J = 7.2 Hz), 7.53 d (1H_{Ar}, J = 7.5 Hz), 8.14 d.d (1H_{Ar}, J = 1.2, 7.8 Hz), 9.20 s (1H, HC=N), 10.28 s (1H, OH). Found, %: C 66.70; H 6.25; N 17.31. $C_{18}H_{20}N_4O_2$. Calculated, %: C 66.65; H 6.21; N 17.21.

Bis{2-[(*E*)-[2-(4-hydroxybutylamino)benzimidazole-1-yl]iminomethyl]phenolato}cobalt(II) (2a). A solution of 0.13 g (0.5 mmol) of cobalt(II) acetate tetrahydrate in 10 mL of methanol was added to a solution of 0.32 g (1 mmol) of compound **1** in a mixture of 30 mL of methanol and 5 mL of DMF, and the mixture was heated under reflux for 1 h. After cooling, the precipitate was filtered off, washed with methanol, and recrystallized from DMF. Yield 0.23 g (65%), brown crystals, mp > 250°C, μ_{eff} 4.3 B.M. (294 K). IR spectrum, ν, cm^{-1}: 3315 br. w (O–H), 1618 s, 1604 s (CH=N). Found, %: C 61.50; H 5.22; N 15.87; Co 8.49. $C_{36}H_{36}CoN_8O_4$. Calculated, %: C 61.27; H 5.43; N 15.88; Co 8.35.

{2-[(*E*)-[2-(4-Hydroxybutylamino)benzimidazole-1-yl]iminomethyl]phenolato}copper(II) acetate (2b) was synthesized in a similar way from 0.32 g (1 mmol) of azomethine **1** in a mixture of 30 mL of methanol and 5 mL of DMF and a methanolic solution of 0.1 g (0.5 mmol) of copper(II) acetate monohydrate. Yield 0.19 g (85%), green crystals, mp > 250°C, μ_{eff} 1.97 B.M. (294 K). IR spectrum, ν, cm^{-1}: 3600–3000 br. w (N–H, O–H), 1675 (C=O), 1622, 1600 s (CH=N). Found, %: C 54.10; H 5.01; N 12.62; Cu 14.18. $C_{20}H_{22}CuN_4O_4$. Calculated, %: C 53.86; H 4.97; N 12.56; Cu 14.25.

ACKNOWLEDGMENTS

The work was performed in the framework of the State order for scientific research (project 3.6105.2017/8.9).

CONFLICT OF INTEREST

No conflict of interest was declared by the authors.

REFERENCES

1. *Comprehensive Coordination Chemistry II*, McCleverty, J.A. and Meyer, T.J., Amsterdam: Elsevier, 2004, vol. 1, p. 125.
2. *Comprehensive Heterocyclic Chemistry III*, Katritsky, A.R., Ramsden, C.A., Scriven, E.F.V., and Taylor, R.J.K., Amsterdam: Elsevier, 2008, vol. 4, p. 143.
3. Küçükgüzel, Ş.G. and Çikla-Süzgün, P., *Eur. J. Med. Chem*., 2015, vol. 97, p. 830. doi 10.1016/j.ejmech.2014.11.033
4. Singh, K., Barwa, M.S., and Tyagi, P., *Eur. J. Med. Chem*., 2006, vol. 41, no. 1, p. 147. doi 10.1016/j.ejmech.2005.06.006
5. Bagihalli, G.B., Avaji, P.G., Patil, S.A., and Badami, P.S., *Eur. J. Med. Chem*., 2008, vol. 43, no. 12, p. 2639. doi 10.1016/j.ejmech.2008.02.013
6. Yu, J.-W., Wang, Y., Wang, Y.-B., and Wang, C.-F., *J. Chem. Res*., 2013, vol. 37, no. 3, p. 164. doi 10.3184/174751913X13605940678869
7. Ko, K.C., Wu, J.-S., Kim, H.J., Kwon, P.S., Bartsch, R.A., Lee, J.Y., and Kim, J.S., *Chem. Commun*., 2011, vol. 47, no. 11, p. 3165. doi 10.1039/C0CC05421F
8. Vasil'chenko, I.S., Kuz'enko, T.A., Divaeva, L.N., Burlov, A.S., Uraev, A.I., Borodkin, G.S., Chepurnoi, P.B., Borodkina, I.G., Beletskii, O.A., Karpov, O.A., Garnovskii, A.D., Shestakova, T.E., Uflyand, I.E., Ikorskii, V.N., Vlasenko, V.G., and Pirog, I.V., *Russ. J. Coord. Chem*., 2007, vol. 33, no. 3, p. 176. doi 10.1134/S1070328407030049
9. Garnovskii, A.D., Ikorskii, V.N., Uraev, A.I., Vasilchenko, I.S., Burlov, A.S., Garnovskii, D.A., Lyssenko, K.A. Vlasenko, V.G., Shestakova, T.E., Koshchienko, Y.V., Kuz'menko, T.A., Divaeva, L.N., Bubnov, M.P., Rybalkin, V.P., Korshunov, O.Yu., Pirog, I.V., Borodkin, G.S., Bren, V.A., Uflyand, I.E., Antipin, M.Yu., and Minkin, V.I., *J. Coord. Chem.*, 2007, vol. 60, no. 14, p. 1493. doi 10.1080/00958970601080365
10. Vasilchenko, I.S., Lyssenko, K.A., Kuz'menko, T.A., Uraev, A.I., Garnovskii, D.A., Divaeva, L.N., and Burlov, A.S., *Mendeleev Commun*., 2015, vol. 25, p. 397. doi 10.1016/j.mencom.2015.09.030

11. Borodkina, I.G., Burlov, A.S., Borodkin, G.S., Chesnokov, V.V., Kuzmenko, T.A., Uraev, A.I., Korshunova, E.V., and Vasil'chenko, I.S., *Russ. J. Gen. Chem*., 2016, vol. 86, no. 4, p. 876. doi10.1134/S1070363216040198

12. Kuznetsova, L.I., Burlov, A.S., Volbushko, N.V., Korshunov, O.Yu., Zaletov, V.G., and Garnovskii, A.D., *Russ. J. Gen. Chem*., 1998, vol. 68, p. 1277.

13. Garnovskii, A.D., Burlov, A.S., Divaeva, L.N., and Antsyshkina, A.S., *Russ. J. Inorg. Chem*., 1996, vol. 41, no. 1, p. 85.

14. Burlov, A.S., Antsyshkina, A.S., Sadikov, G.G., Divaeva, L.N., Garnovskii, A.D., and Sergienko, V.S., *J. Coord. Chem*., 2000, vol. 26, no. 9, p. 648.

15. Garnovskii, A.D., Garnovskii, D.A., Vasil'chenko, I.S., Burlov, A.S., Sadimenko, A.P., and Sadekov, I.D., *Russ. Chem. Rev*., 1997, vol. 66, no. 5, p. 389. doi 1070/RC1997v066n05ABEH000258

16 Vasil'chenko, I.S., Kuz'menko, T.A., Shestakova, T.E., Borisenko, R.N., Divaeva, L.N., Burlov, A.S., Borisenko, N.I., Uflyand, I.E., and Garnovskii, A.D., *Russ. Coord. Chem*., 2005, vol. 31, no. 10, p. 747. doi 10.1007/s11173-005-0163-6

17. Barszcz, B., Jablonska-Wawrzycka, A., Stadnicka, K., and Jezierska, J., *Polyhedron*, 2008, vol. 27, no. 17, p. 3500. doi 10.1016/j.poly.2008.07.038

18. Barszcz, B., Głowiak, T., and Jezierska, J., *Polyhedron*, 1999, vol. 18, no. 27, p. 3713. doi 10.1016/S0277-5387(99)00311-3

19. Barszcz, B., Glowiak, T., and Detka, K., *Polyhedron*, 2003, vol. 22, no. 10, p. 1329. doi 10.1016/S0277-5387(03)00130-X

20. Palion-Gazda, J., Machura, B., Klemens, T., and Kłak, J., *Polyhedron*, 2014, vol. 81, p. 465. doi 10.1016/j.poly.2014.06.020

21. Zhou, Y.-L., Liang, H., and Zeng, M.-H., *Acta Crystallogr., Sect. E*, 2010, vol. 66, p. 188. doi 10.1107/S1600536810002126

22. Zheng, L.-L., Leng, J.-D., Herchel, R., Lan, Y.-H., Powell, A.K., and Tong, M.-L., *Eur. J. Inorg. Chem*., 2010, no. 15, p. 2229. doi 10.1002/ejic.201000222

23. Goodgame, M., Holt, S.D., Piggott, B., and Williams, D.J., *Inorg. Chim. Acta*, 1985, vol. 107, no. 49, p. 49. doi 10.1016/S0020-1693(00)80689-1

24. Piggott, B., Hursthouse, M.B., Thornton, P., and Walker, N.P.C., *Polyhedron*, 1988, vol. 7, no. 4, p. 323. doi 10.1016/S0277-5387(00)80474-X

25. Huang, L., Zhong, A.-G., Chen, D.-B., and Liang, H.-D., *J. Mol. Struct., 2009*, vol. 922, no. 1–3, p. 135. doi 10.1016/j.molstruc.2008.12.056.

26. Zhou, Y.-L., Liang, H., and Zeng, M.-H., *Acta Crystallogr., Sect. E*, 2010, vol. 66, p. 189. doi 10.1107/S1600536810002114

27. Becke, A.D., *J. Chem. Phys*., 1993, vol. 98, no. 7, p. 5648. doi 10.1063/1.464913

28. Lee, C., Yang, W., and Parr, R.G., *Phys. Rev. B*, 1988, vol. 37, no. 2, p. 785. doi 10.1103/PhysRevB.37.785

29. Schaefer, A., Huber, C., and Ahlrichs, R., *Chem. Phys*., 1994, vol. 100, p. 5829. doi10.1063/1.467146

30. Ivanova, T., Naumkin, A., Sidorov, A., Eremenko, I., and Kiskin, M., *J. Electron Spectrosc. Relat. Phenom*., 2007, vols. 156–158, p. 200. doi 10.1016/j.elspec.2006.12.005

31. Rakitin, Yu.V. and Kalinnikov, V.T., *Sovremennaya magnetokhimiya* (Modern Magnetochemistry), St. Petersburg: Nauka, 1994, p. 276.

32. Ravel, B. and Newville, M., *J. Synchrotron Radiat*., 2005, vol. 12, p. 537. doi 10.1107/S0909049505012719

33. Zabinski, S.I., Rehr, J.J., Ankudinov, A., Albers, R.C., and Eller, M., *J. Phys. Rev. B*, 1995, vol. 52, p. 2995. doi 10.1103/PhysRevB.52.2995

34. *SMART and SAINT*. Release 5.0. Area Detector Control and Integration Software. Madison, Wis, US: Bruker AXS, 1998.

35. Sheldrick, G.M., *SADABS*. A Program for Exploiting the Redundancy of Area-detector X-Ray Data, Göttingen, Germany: Univ. Göttingen, 1999.

36. Sheldrick, G.M., *Acta Crystallogr., Sect. A*, 2008, vol. 64, no. 1, p.112. doi 10.1107/S0108767307043930

37. Spek, L., *J. Appl. Crystallogr*., 2003, vol. 36, no. 1, p. 7. doi 10.1107/S0021889802022112

38. Morkovnik, A.S., Kuz'menko, T.A., Divaeva, L.N., Koshchienko, Y.V., Anisimova, V.A., Bogoslavtseva, M.V., Spasov, A.A., Kucheryavenko, A.F., Rogova, N.V., Kuznetsova, V.A., Chepljaeva, N.I., Solovyova, O.A., Taran, A.S., Vorobiev, E.S., Aleshin, D.A., Sirotenko, V.S., Gajdukova, K.A., and Kuzmina, L.G., *Russ. Chem. Bull.,* 2015, vol. 64, no. 11, p. 2622. doi.1007/s11172-015-1200-3